12th International Symposium on Turbulence and Shear Flow Phenomena (TSFP12)
Osaka, Japan (Online), July 19-22, 2022

SCALING LAWS AND WALL-ATTACHED STRUCTURES IN A SUPERSONIC TURBULENT CHANNEL FLOW

Hyeon Gyu Hwang
Department of Mechanical Engineering
UNIST
50 UNIST-gil, Eonyang-eup, Ulsan, 44919, Korea
hyunq92@unist.ac.kr

Jae Hwa Lee
Department of Mechanical Engineering
UNIST
50 UNIST-gil, Eonyang-eup, Ulsan, 44919, Korea
jhlee06@unist.ac.kr

Jinyul Hwang
School of Mechanical Engineering
PNU
2 Busandaehak-ro 63beon-gil, Geumjeong-gu, Busan, 46241, Korea
jhwang@pnu.ac.kr

Ji-Hoon Kang
Division of National Supercomputing
KISTI
245 Daehak-ro, Yuseong-gu, Daejeon, 34141, Korea
jhkang@kisti.re.kr

Hyung Jin Sung
Department of Mechanical Engineering
KAIST
291 Daehak-ro, Yuseong-gu, Daejeon, 34141, Korea
hjsung@kaist.ac.kr

ABSTRACT

To establish integrating explanation for characteristics of compressible wall-bounded turbulence, scaling laws and relevant turbulent coherent structures in compressible wall-bounded turbulence are investigated in light of Townsend's attached-eddy hypothesis. Using data of direct numerical simulation of supersonic turbulent channel flow between isothermal walls, we verified the scaling laws for mean velocity and Reynolds stresses, which can be predicted by attached-eddy hypothesis in a unified way. The transformed mean velocity profiles and the Reynolds stresses using semi-local scale supports the predicted scaling laws at certain extent. However, complete logarithmic dependence is not achieved due to relatively low-Reynolds number or insufficient scale separation, especially for streamwise normal stress. In search of coherent structures responsible for the logarithmic dependence of the turbulent statistics, wall-attached structures of velocity fluctuations are extracted from instantaneous flow fields. Reconstructed flow field from wall-attached self-similar structures fits more closer to the logarithmic variation. With these findings, we have provided the convincing evidence for the validity of the scaling laws and the existence of coherent structures corresponding the attached-eddy hypothesis for the compressible wall-bounded turbulence.

INTRODUCTION

Scaling laws for statistical features of wall-bounded turbulence has been an important issue since they are considered as building blocks for understanding the characteristics of the wall-bounded turbulence. Furthermore, given that the wall-bounded turbulence consists of coherent structures (i.e., eddies) which naturally occur across a wide range of length scales and are considered as responsible for the relevant scaling laws, efforts has been devoted to investigation of such coherent structures because it has been a foundation for modelling and control strategies of the wall-bounded turbulence. Along with these principal thoughts, the study of the scaling laws and the coherent structures has started from the study of incompressible wall-bounded turbulence, due to relatively simple condition of constant fluid properties, while the study of compressible wall-bounded turbulence is preceded by, and hence, takes its root in the incompressible counterpart.

From the classical point of view, the presence of a wall naturally enforces multiscale characteristics on turbulence above the wall, with length scale ranging from viscous length scale δ_v to flow thickness δ. The scale separation between these distinct length scales is usually expressed as friction Reynolds number, $Re_\tau=\delta/\delta_v$. Emerging with sufficient scale separation (high Re_τ), logarithmic variation of mean velocity profiles is recognized as a cornerstone for the wall-bounded turbulence. This region, so called as logarithmic region, occurs at $\delta_v<<y<<\delta$ (y is distance from the wall), and it is equivalent to the condition of the sufficient scale separation. In essence, characteristic velocity scale is friction velocity $u_\tau=(\tau_w/\rho)^{1/2}$ (τ_w is wall-shear stress and ρ is density) and any geometric length scale is proportional to distance from the wall, y (Marusic *et al*., 2013).

In this context, Townsend (1976) conjectured that the length scales of energy-containing eddies in the logarithmic region are scaled by their position (y), and thus, they extend to the wall, which is called Townsend's attached-eddy hypothesis (AEH). Based on the AEH by Townsend (1976), Perry and Chong (1982) proposed the statistical description of logarithmic region in wall-bounded turbulent flows such that hierarchies of geometrically self-similar eddies are superpositioned with their population inversely proportional to their length scale (y). The proposed representation and following deductions, which is called as attached-eddy model (AEM), lead to important scaling laws for

the wall-bounded turbulence, such as logarithmic variation of mean velocity and Reynolds stresses for wall-parallel components, as well as their spectral imprint of k^{-1} scaling (k is wavenumber). Further refinement of attached-eddy model has been achieved through the following studies (Perry *et al.*, 1986; Perry and Marusic, 1995 and so on). Recently, evidence of the AEH (or the AEM) has been substantiated by observations for co-existence of logarithmic variations of mean velocity and normal stresses in high-Reynolds-number flow fields with high-fidelity (Hultmark *et al.*, 2012; Marusic *et al.*, 2013; Lee and Moser 2015), and hence its significance is more increasing.

In last decades, the efforts have been devoted in order to identify the coherent structures corresponding to the AEH. Although several studies (del Álamo *et al*., 2006; Lozano-Durán *et al*., 2012) provided the existence of self-similar motions in physical space, whether they are responsible for the formation of logarithmic variation have not been elucidated. Among the relevant studies, studies by Hwang and Sung (2018; 2019) found that the wall-attached clusters of streamwise velocity fluctuations are not only geometrically self-similar but also have population density following the hierarchical length scale distribution. Furthermore, they successfully showed a reconstructed flow field from the identified structures displays clear logarithmic variations of the statistics even at relatively low- to moderate-Reynolds number, suggesting the identified structures as prime candidates for the coherent structures corresponding the AEH.

On the other hand, the established scaling laws for mean velocity and Reynolds stresses in the incompressible wall-bounded turbulence is not directly affordable for the compressible wall-bounded turbulence because properties such as thermodynamic properties (e.g., temperature, density and pressure) are not constant. One might expect that the variations in properties would significantly alter various aspect of wall-bounded turbulence. According to Morkovin's hypothesis (MH), at moderate Mach number, compressibility effect of density fluctuation on turbulence is small, and essential dynamics closely follow those of incompressible flow (Morkovin, 1962). Hereafter, compressible wall-bounded turbulence only indicates the moderate Mach number flow (i.e., non-hypersonic flow) if without any specification.

Encouraged by the principle of the MH, the scaling laws for the compressibile wall-bounded turbulence have been established via compressibility transformation, which casts the compressible turbulent statistics to incompressible counterpart. Accordingly, the logarithmic variations for mean velocity and wall-parallel components of the Reynlolds stresses (AEH) are expected through the transformations (Smits and Dussage, 2006). Although van-Driest transformation and Morkovin's scaling, in general, are agreed upon based on large volume of experimental data (Fernholz and Finley, 1980; Smits and Dussage, 2006), their accuracy has been questioned due to uncertainty in measurment. This issue was resolved by performing direct numerical simulation of the compressible flow, and modified transformations are also suggested (Trettel and Larsson, 2016; Huang *et al.*, 1995) for strong wall heat transfer conditions. However, the DNSs of the compressible flow have been performed at relatively low-to-moderate Reynolds number limited by computational cost, and complete logarithmic variations for the turbulence statistics, especially for the streamwise Reynolds stresses, are not observed due to insufficent scale separations.

On the other hand, in similar context with the incompressible counterpart, several studies have devoted efforts to elucidate the existence of self-similar coherent structures in the sense of the AEH. Pirozzoli (2012) and Modesti and Pirozzoli (2016; 2019) proposed an appropriate length scales for spanwise width of spatial correlation and spanwise wavelength at peak of energy spectra of stremwise velocity fluctuation in compressible flow of canonical geometries. In their studies, the proposed length scales showed good scaling accuracy in overall outer layer with reasonable Mach number range, and it is indicates increasing trends of the spanwise length scales for the turbulent motions with the wall-normal locations. Although these studies successfully took account of the compressibility effects on the length scales of the turbulent motions, and found the presence of self-similar motions in the compressible wall-bounded turbulence, it has not revealed for how they contribute to the suggested scaling laws.

The objective of present study is to establish integrating explanation for characteristics of compressible wall-bounded turbulence. To this end, scaling laws and relevant turbulent coherent structures in compressible wall-bounded turbulence are investigated in terms of the AEH. We verify the predicted scaling behaviors using data of direct numerical simulation of supersonic turbulent channel flow between isothermal walls at moderate Reynolds number. In search of coherent structures responsible for the logarithmic variation of the turbulent statistics, wall-attached structures of velocity fluctuations are identified by implementing the method of Hwang and Sung (2018; 2019) and their characteristics are investigated.

NUMERICAL METHODS

Direct numerical simulation of supersonic turbulent channel flow between isothermal wall at Re_b=24000 and Ma_b=1.5 (where subscript b denotes bulk variables) is performed by solving governing equations of compressible perfect gas with the numerical schemes of Bernardini *et al.* (2020). Based on the wall variables (u_τ and δ_v) semi-local variables (u_τ^* and δ_v^*), the flow's friction Reynolds number $Re_\tau=h/\delta_v$ (h is channel half-height) and semi-local Reynolds number $Re_\tau^*=h/\delta_v^*$ are 1390 and 930, respectively, and it is denoted as C930. Throughout the present study, x, y and z indicate streamwise, wall-normal and spanwise directions, respectively, and u, v and w are velocity components for each direction. Computational domain is set as $L_x \times L_y \times L_z = 10\pi h \times 2h \times 3\pi h$, which is expected to be sufficiently long to accommodate large- and very-large scale motions (Kim and Adrian, 1999; Ganapathisubramani *et al*., 2006). Uniform grid spacing is implemented in the streamwise and spanwise direction, while grids are clustered toward the walls using hyperbolic tangent mapping function. Grid resolutions in each direction based on wall variable (Δx^+, Δy^+ and Δz^+) are set as 14.31, 0.16~9.41 and 7.38, respectively. For the comparison, DNS data of incompressible turbulent channel flow at Re_τ=930 (Lee *et al.* 2014) are employed, which are denoted as I930. The numerical details for DNS of I930 is referred to Lee *et al.* (2014).

For averaging methods, it is noted that $\langle f \rangle$ and f' refer to Reynolds-averaged and fluctuating quantities, while $\{f\}=\langle \rho f \rangle / \langle \rho \rangle$ (ρ is density) and f'' denote Favre-averaged and fluctuating quantities. And superscript + and * indicate quantities scaled by wall and semi-local variables, respectively. It is noted that, for incompressible flow, both scalings are identical by definition and transformation has no effects on quantities due to constant properties.

SCALING LAWS OF COMPRESSIBLE WALL-BOUNDED TURBULENCE

Scaling laws for mean velocity profile for the compressible wall-bounded flow is expressed in form of gradient as below (1)

$$\frac{d\{u\}}{dy} = \frac{u_\tau^*}{\kappa y} \tag{1}$$

, where κ is the von-Kármán constant. This scaling law was derived from extension of mixing length theory (van-Driest 1951) or law of the wall (Bradshaw 1994) with assumption of the existence of constant stress region close to the wall and consideration of the mean density variation. In their studies, the scaling constant κ is assumed to be identical with that of the incompressible counterpart.

In investigating the scaling law for mean velocity (1) based on the obtained DNS data, compressibility transformations are implemented. As following Modesti and Pirozzoli (2016; 2019), the compressibility transformations for the distribution of mean velocity are casted to forms of integral. The transformations for the wall-normal coordinate and the mean velocity are expressed as $y_\mathrm{T} = \int_0^y f_\mathrm{T} dy$ and $\{u\}_\mathrm{T} = \int_0^{\{u\}} g_\mathrm{T} d\{u\}$, respectively. Here, subscript T denotes transformed quantities and f_T and g_T are transformation kernels. By changing the variable of integration with the chain rule, the formula for $\{u\}_\mathrm{T}$ is rearranged as $\{u\}_\mathrm{T} = \int_0^y g_\mathrm{T}\{u\}_y dy$ ($\{u\}_y$ denotes $d\{u\}/dy$). Then, using their gradients (i.e., dy_T/dy and $d\{u\}_\mathrm{T}/dy$), $d\{u\}_\mathrm{T}/dy_\mathrm{T}$ can be expressed as below (2).

$$\frac{d\{u\}_\mathrm{T}}{dy_\mathrm{T}} = \frac{g_\mathrm{T}}{f_\mathrm{T}}\frac{d\{u\}}{dy} \tag{2}$$

Whilst, if profile of $\{u\}_\mathrm{T}$ shows logarithmic variation in the transformed coordinate (y_T), the relation for the $d\{u\}_\mathrm{T}/dy_\mathrm{T}$ follows as

$$\frac{d\{u\}_\mathrm{T}}{dy_\mathrm{T}} = \frac{u_\tau}{\kappa_c y} \tag{3}$$

, where κ_c is scaling constant, but not to be determined yet, since it is not known *a priori* whether scaling constant κ_c is same with the von-Karman constant κ. Here, the velocity scale for $\{u\}_\mathrm{T}$ in (3) is u_τ since compressibility transformations in use will adopt constant variable (i.e., wall variables). Now, Equating (2) and (3) yields the relation for the actual (or untransformed) mean velocity gradient (4).

$$\frac{d\{u\}}{dy} = \left(\frac{g_\mathrm{T}}{f_\mathrm{T}}\right)^{-1}\frac{u_\tau}{\kappa_c y_\mathrm{T}} \tag{4}$$

It is stressed that relation (4) is valid only when the transformed mean velocity follows logarithmic variation (3), while scaling property of $d\{u\}/dy$ expressed by (4) depends on the constitution of compressibility transformation in use (i.e., kernel f_T and g_T). From this procedure, one can obtain straight information about the actual mean velocity $\{u\}$ from scaling properties of the transformed velocity. For the present analysis, we investigate transformed mean velocity profiles of $\{u\}_\mathrm{D}(y_\mathrm{D})$ by van-Driest (1951) and $\{u\}_\mathrm{TL}(y_\mathrm{TL})$ by Trettel and Larsson (2016), as well as untransformed (actual) mean velocity $\{u\}_\mathrm{un.}=\{u\}$. The sets of the transformation kernels for the van-Driest transformation (5) and the Trettel and Larsson transformation (6) are described below.

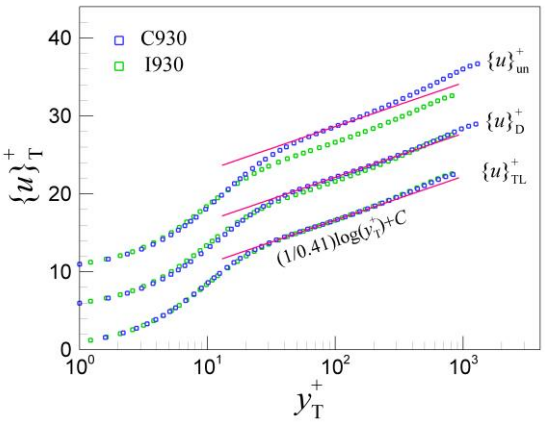

Figure 1. Mean velocity profiles for C930 (blue symbols) and I930 (green symbols): (upper) untransformed velocity, $\{u\}_\mathrm{un}^+$ (middle) D-transformation $\{u\}_\mathrm{D}^+$ and (lower) TL-transformation $\{u\}_\mathrm{TL}^+$. Former two profiles are displaced by $\Delta\{u\}_\mathrm{T}^+=5$. Colored straight lines are added as guides for logarithmic variation.

$$\left.\begin{aligned} f_D &= 1 \\ g_D &= \left(\langle\rho\rangle/\langle\rho_w\rangle\right)^{1/2} \end{aligned}\right\} \tag{5}$$

$$\left.\begin{aligned} f_\mathrm{TL} &= \left(\frac{\langle\mu_w\rangle}{\langle\mu\rangle}\right)\left(\frac{\langle\rho\rangle}{\langle\rho_w\rangle}\right)^{1/2}\left[1+\frac{1}{2}\frac{1}{\langle\rho\rangle}\frac{d\langle\rho\rangle}{dy}y-\frac{1}{\langle\mu\rangle}\frac{d\langle\mu\rangle}{dy}y\right] \\ g_\mathrm{TL} &= \left(\frac{\langle\rho\rangle}{\langle\rho_w\rangle}\right)^{1/2}\left[1+\frac{1}{2}\frac{1}{\langle\rho\rangle}\frac{d\langle\rho\rangle}{dy}y-\frac{1}{\langle\mu\rangle}\frac{d\langle\mu\rangle}{dy}y\right] \end{aligned}\right\} \tag{6}$$

In figure 1, profiles of mean velocities for C930 and I930 are illustrated. As previously reported, an excellent accuracy for TL-transformation is observed where $\{u\}_\mathrm{TL}(y_\mathrm{TL})$ perfectly collapse onto the profile of I930, and hence, it shows logarithmic variation with the slope of $1/\kappa_c=1/0.41$. Since $\{u\}_\mathrm{TL}(y_\mathrm{TL})$ satisfies (3), it is possible to use (4) to determine the property of $d\{u\}/dy$. Direct substitution of f_TL, g_TL, y_TL and κ (also found in scaling law of dissipation) into f_T, g_T, y_T and κ_c in (4) exactly leads to $d\{u\}/dy \sim u_\tau^*/\kappa y$. Next, the profile of $\{u\}_\mathrm{D}(y_\mathrm{D})$ does not collapse onto the I930, and this failure is not expected to be recovered even for a comparison of matching Re_τ. As noted by previous studies (Modesti and Pirozzoli, 2016; Yao and Hussain, 2020), however, profile still follows logarithmic variation with the identical slope of $1/\kappa_c=1/0.41$ with a certain extent. Then, the identical approach with $\{u\}_\mathrm{TL}(y_\mathrm{TL})$ can be applied for $\{u\}_\mathrm{D}(y_\mathrm{D})$ and it deduces $d\{u\}/dy \sim u_\tau^*/\kappa y$. Therefore, both transformation results resolve to same conclusion leading to the scaling law (1) and the successful transformations are consistent with the MH. On the other hand, a region for the logarithmic variation with the slope of $1/\kappa_c=1/0.41$ for $\{u\}_\mathrm{un}$ is substantially narrowed (around at $y^+=100$) so that the presence of the logarithmic region is not certain. According to (1) consistent with present findings, it is predictable because the scaling for mean velocity will fail when using constant value of u_τ, instead of u_τ^* which varies with y.

On the other hand, the scaling laws for the Reynolds stresses (7-9) are predicted by the AEH and the Morkovin's scaling (Smits and Dussage, 2006), the latter alternating the velocity scale for the turbulent motions from u_τ to u_τ^*.

$$\{u''u''\}^* = B_1 - A_1 \log\left(\frac{y}{\delta}\right) \quad (7)$$

$$\{w''w''\}^* = B_2 - A_2 \log\left(\frac{y}{\delta}\right) \quad (8)$$

$$\{v''v''\}^* = B_3 \quad (9)$$

Here, A_i (i=1, 2, 3) and B_j (j=1, 2) are constant. According to the prediction of the AEH, scaling by inner variables fails for wall-parallel components of Reynolds stresses due to the superposition of the energy-containing eddies having finite slip velocity near the wall. While the wall-normal component is constant due to restriction by the impermeable boundary condition (Townsend 1976; Perry and Chong 1982).

Figure 2 provides profiles of Reynolds stress for C930 and I930 in inner and outer coordinates. The profiles in inner coordinates adopt scaling by semi-local variables (Huang *et al.*, 1995) and the profiles collapse well throughout whole layer as matching the semi-local Reynolds number (Re_τ^*) between C930 and I930, except increased streamwise intensities near the wall. While the profiles in the outer coordinate, consistent with the Morkovin's scaling, well matched in the outer layer even though the frictional Reynolds numbers (Re_τ) differ.

For each component, the scaling law of (8) for the spanwise components is observed. For the incompressible case, this behavior is reported from previous study (Lee and Moser, 2015) and it starts to emerge at $Re_\tau \approx 1000$ and, for the compressible case, scaling law of (8) is also observed from similar simulation results by Modesti and Pirozzoli (2016) and Yao and Hussain (2020). Besides, the scaling law of (9) for the wall-normal components are confirmed, also. This behavior is easily observable in numerous literatures. However, the logarithmic variation for the streamwise components (7) are not found for both cases. Considering that the logarithmic variation of streamwise normal stress is observable at much higher Reynolds number in the incompressible flows (Hultmark *et al.*, 2012; Marusic *et al.*, 2013), the logarithmic dependence for the streamwise normal stress is remain unclear. But hopefully, the scaling by semi-local frictional velocity u_τ^* is very successful at low Reynolds number, we can only expect the logarithmic variation of streamwise normal stress is observable at much higher Reynolds number.

Although the above results showed that, at some extent, the turbulent statistics follow the scaling laws of (1) and (8-9) for the compressible wall-bounded turbulence, using the compressibility transformations and the semi-local variables, rigorous logarithmic dependence are not achieved based on indicator function, especially for the streamwise Reynolds stress, due to relatively low-Reynolds number. Furthermore, even if the scaling laws (1) and (7-9) are valid, coherent structures

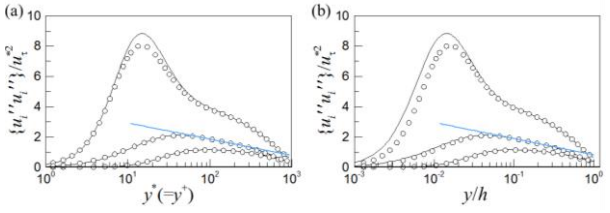

Figure 2. Reynolds stresses profiles in (a) inner and (b) outer coordinates. Lines in each panel are profiles for C930 while symbols indicate those for I930. Colored straight lines are added as guides for logarithmic variation for the spanwise components

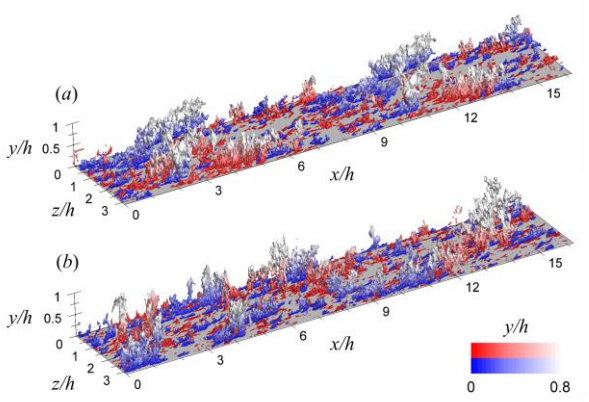

Figure 3. Iso-surfaces of identified wall-attached structures of streamwise velocity fluctuations in an instantaneous flow field: (*a*) I930 and (*b*) C930. Red and Blue colors indicate positive and negative fluctuations, respectively, and colors fade out as *y*/*h* increases.

contributing to these scaling laws are not elucidated for the compressible wall-bounded turbulence, yet.

WALL-ATTACHED STRUCTURES OF VELOCITY FLUCTUATIONS

The other goal of the present study is to identify actual coherent structures within random instantaneous flow fields, which correspond to the AEH and contribute to the scaling laws. To this end, clusters of velocity fluctuations are identified through the methodology suggested by Hwang and Sung (2018; 2019). The clusters of velocity fluctuations are defined as the groups of connected points satisfying $u''>+\alpha\{u''u''\}^{1/2}$ or $u''<-\alpha\{u''u''\}^{1/2}$, where α=1.6 based on percolation theory. Owing to the advantage of DNS, three-dimensional spatial information of the identified structures is accessible, and assigned to each of structures. Based on their minimum distance from the wall, the identified structures are classified into wall-attached and detached structures. Examples of the wall-attached structures for C930 and I930 are provided in figure 3, and qualitative similarity is found supporting the validity of the MH.

The dimensions of individual structures are determined by dimensions of their bounding boxes, and length, height and width of structures are denoted as l_x, l_y and l_z, respectively. Figure 4 illustrates the self-similarity nature of the identified structures as mean length $\langle l_x \rangle$ and width $\langle l_z \rangle$ follow $\langle l_x \rangle \sim l_y^{0.74}$ and $\langle l_z \rangle \sim l_y$, respectively. In addition, the number density of the structures per unit area (n_s) also showed their population following the hierarchical length scale distribution (inversely proportional to l_y), which is not shown here. These results indicates that the characteristics of the identified structures is consistent with the AEH.

According to the AEH, the superposition of geometrically self-similar hierarchies leads to the logarithmic variation of the turbulent statistics. To determine whether the identified structures exhibit the logarithmic variation of the turbulent statistics in the sense of the AEH, statistical flow field is reconstructed from motions carried by the extracted wall-attached structures showing both the self-similarity and the hierarchical length scale distribution, and detailed definition for reconstructed flow field can be found in Hwang and Sung (2018; 2019). Figure 5(a) shows the logarithmic dependence of the reconstructed $\{u''u''\}_{as}$ from the identified structures, normalized

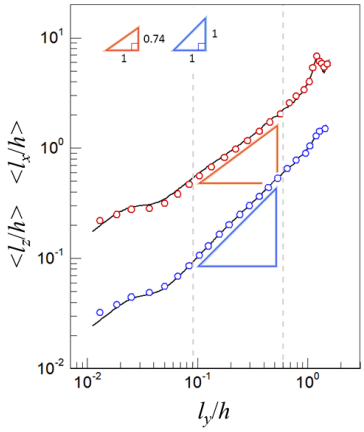

Figure 4. Variations of ensemble-averaged length $<l_x>$ (upper) and width $<l_z>$ (lower) of the wall-attached structures with respect to its height. Lines are for C930 while symbols represent the I930. Colored right-angled triangles are added as guides.

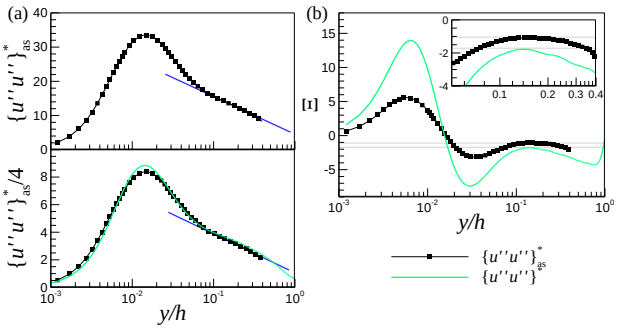

Figure 5. (a) (upper) Streamwise Reynolds stress reconstructed from the identified wall-attached structures $\{u''u''\}_{as}$ based on Morkovin's scaling and (lower) comparison between distribution of the reconstructed stress $\{u''u''\}_{as}$ and the actual stress $\{u''u''\}$. Blue straight lines are added as guides for the logarithmic variations. (b) Indicator functions $\Xi=yd\{u''u''\}^*_{as}/dy$ for estimating logarithmic variation. In each panel, comparison is done as $\{u''u''\}^*_{as}$ being reduced by factor of 4.

by u_τ^*. Here, it is noted that due to the definition of the identified structures (intense u'' by α=1.6) and $\{u''u''\}_{as}$, the magnitude of $\{u''u''\}_{as}$ are much greater than that of $\{u''u''\}$. Since the objective of the present study is to identify coherent structures contributing to the scaling laws in terms of the AEH, comparison here is done by reducing magnitudes as factor of 4, as focusing the logarithmic variation, rather than the actual magnitude. In this way, lower panel of figure 5(a) again confirms the logarithmic dependence of $\{u''u''\}_{as}$. which is absent in the actual streamwise stress $\{u''u''\}$. The logarithmic dependence can be analysed using indicator function $\Xi=yd\{u''u''\}^*_{as}/dy$, where a plateau region indicates complete logarithmic dependence. In accordance with the figure 5(a), indicator function for $\{u''u''\}_{as}$ in figure 5(b) has been much flattened than that of $\{u''u''\}$, and it deviates from constant value much more gradually.

Additionally, similar analysis for the mean velocity for the motions carried by the identified structures ($\{u\}_{as}$) also revealed more clear logarithmic dependence for the reconstructed flow field (not shown here). As a result, we have confirmed the presence of the coherent structures contributing to the scaling laws for the compressible flow. And it is conjectured that the observed logarithmic dependences in the reconstructed flow-fields at the moderate-Reynolds number seem to be masked in the actual mean velocity $\{u\}$ and/or stress distribution $\{u''u''\}$ by insufficient scale separation or contamination of other scales.

CONCLUSION

The turbulent statistics obtained from direct numerical simulation of supersonic turbulent channel flow between isothermal walls showed the existence of y-scaling region with the velocity scale to be u_τ^*. In this region, the transformed mean velocity profiles showed logarithmic variation, while the spanwise and wall-normal components of the Reynolds stresses followed the prediction by the AEH. However, due to relatively low-Reynolds number or insufficient scale separation, the complete logarithmic dependence is not achieved. Especially, the streamwise normal stress is far from the prediction of the AEH. In search of the coherent structures responsible for the logarithmic dependence of the turbulent statistics, reconstructed flow field from the wall-attached self-similar structures showed clear logarithmic variation for the streamwise normal stresses, as manifesting their primary role for the formation of the scaling laws. Through the present study, the integrating explanation for the characteristics of the compressible wall-bounded turbulence is established as providing the supporting evidence of the AEH for the compressible wall-bounded turbulence.

REFERENCE

del Álamo, J. C., Jiménez, J., Zandonade, P., and Moser, R. D., 2006, "Self-similar vortex clusters in the turbulent logarithmic region", *Journal of Fluid Mechanics*, Vol. 561, pp. 329–358.

Bernardini, M., Modesti, D., Salvadore, F., and Pirozzoli, S., 2021, "STREAmS: A high-fidelity accelerated solver for direct numerical simulation of compressible turbulent flows", *Computer Physics Communications*, Vol. 263, 107906.

Bradshaw, P., 1994, "Turbulence: The chief outstanding difficulty of our subject", *Experiments in Fluids*, Vol. 16, pp. 203–216.

van Driest, E., 1951, "Turbulent boundary layer in compressible fluids", *Journal of the Aeronautical Sciences*, Vol. 18, pp. 145-160.

Fernholz, H. H., and Finley, P. J., 1980, "A critical commentary on mean flow data for two-dimensional compressible turbulent boundary layers", AGARDograph 253.

Ganapathisubramani, B., Clemens, N. T., and Dolling, D. S., 2006, "Large-scale motions in a supersonic turbulent boundary layer", *Journal of Fluid Mechanics*, Vol. 556, pp. 271–282.

Huang, P., Coleman, G., and Bradshaw, P., 1995, "Compressible turbulent channel flows: DNS results and modelling", *Journal of Fluid Mechanics*, Vol. 305, pp. 185-218.

Hultmark, M., Vallikivi, M., Bailey, S. C. C., and Smits, A. J., 2012, "Turbulent pipe flow at extreme Reynolds numbers", *Physics Review Letters*, Vol. 108(9), 094501.

Hwang J., and Sung, H. J., 2018, "Wall-attached structures of velocity fluctuations in a turbulent boundary layer", *Journal of Fluid Mechanics*, Vol. 856, pp. 958–983.

Hwang, J., and Sung, H. J., 2019, "Wall-attached clusters for the logarithmic velocity law in turbulent pipe flow", *Physics of Fluids*, Vol. 31 (5), 055109.

Kim, K. C., and Adrian, R. J., 1999, "Very large-scale motion in the outer layer", *Physics of Fluids*, Vol. 11(2), pp. 417–422.

Lee, J., Lee, J. H., Choi, J.-I., and Sung, H. J., 2014, "Spatial organization of large-and very-large-scale motions in a turbulent channel flow", *Journal of Fluid Mechanics*, Vol. 749, pp. 818–840.

Lee, M., and Moser, R. D., 2015, "Direct numerical simulation of turbulent channel flow up to $Re_\tau \approx 5200$", *Journal of Fluid Mechanics*, Vol. 774, pp. 395–415.

Lozano-Durán, A., Flores, O., and Jiménez, J., 2012, "The three-dimensional structure of momentum transfer in turbulent channels", *Journal of Fluid Mechanics*, Vol. 694, pp. 100–130

Marusic, I., Monty, J. P., Hultmark, M., and Smits, A. J., 2013, "On the logarithmic region in wall turbulence", *Journal of Fluid Mechanics*, Vol. 716, R3

Modesti, D., and Pirozzoli, S., 2016, "Reynolds and Mach number effects in compressible turbulent channel flow", *International Journal of Heat and Fluid Flow*, Vol. 59, pp. 33–49.

Modesti, D., and Pirozzoli, S., 2019, "Direct numerical simulation of supersonic pipe flow at moderate Reynolds number", *International Journal of Heat and Fluid Flow*, Vol. 76, pp. 100–112.

Morkovin, M., 1962, "Effects of compressibility on turbulent flows", Mécanique de la Turbulence. A. Favre, pp. 367–380.

Perry, A. E., and Chong, M. S., 1982, "On the mechanism of wall turbulence", *Journal of Fluid Mechanics*, Vol. 119, pp. 173–217.

Perry, A. E., Henbest, S., and Chong, M. S., 1986, "A theoretical and experimental study of wall turbulence", *Journal of Fluid Mechanics*, Vol. 165, pp. 163–199.

Perry, A. E., and Marusic, I., 1995, "A wall-wake model for the turbulence structure of boundary layers. Part 1. Extension of the attached eddy hypothesis", *Journal of Fluid Mechanics*, Vol. 298, pp. 361–388.

Pirozzoli, S., 2012, "On the size of the energy-containing eddies in the outer turbulent wall layer", *Journal of Fluid Mechanics*, Vol. 702, pp. 521–532.

Smits, A. J., and Dussage, J. P., 2006, *Turbulent Shear Layers in Supersonic Flow*. Springer.

Townsend, A. A., 1976, *The structure of turbulent shear flow*. Cambridge University Press.

Trettel, A. and Larsson, J., 2016, "Mean velocity scaling for compressible wall turbulence with heat transfer", *Physics of Fluids*, Vol. 28 (2), 026102.

Yao, J., and Hussain, F., 2020, "Turbulence statistics and coherent structures in compressible channel flow", *Physical Review Fluids*, Vol. 5, 084603.